Pre-ozonation coupled with forward osmosis with fertilizer as draw solution for simultaneous wastewater treatment and agricultural irrigation

Fu Yang, Qianyun Wang, Xingbao Wang, Yuanyuan Shan, Chongde Wu, Rongqing Zhou, Nicolas Hengl, Frédéric Pignon, Yao Jin

Pre-ozonation coupled with forward osmosis with fertilizer as draw solution for simultaneous wastewater treatment and agricultural irrigation

Fu Yang [a,b], Xingbao Wang [c,*], Yuanyuan Shan [d], Chongde Wu [a,b], Rongqing Zhou [a,b], Nicolas Hengl [e], Frederic Pignon [e], Yao Jin [a,b,*]

[a] College of Biomass Science and Engineering, Sichuan University, Chengdu 610065, China.

[b] Key Laboratory for Leather and Engineering of the Education Ministry, Sichuan University, Chengdu 610065, China.

[c] State Key Laboratory of Clean and Efficient Coal Utilization, Taiyuan University of Technology, Taiyuan 030024, China.

[d] Institute of New Carbon Materials, College of Materials Science and Engineering, Taiyuan University of Technology, Taiyuan, 030024, China.

[e] Univ. Grenoble Alpes, CNRS, Grenoble INP (Institute of Engineering Univ. Grenoble Alpes), LRP, F-38000 Grenoble, France

* Corresponding author at:

State Key Laboratory of Clean and Efficient Coal Utilization, Taiyuan University of Technology, Taiyuan 030024, China. (Xingbao Wang)

College of Biomass Science and Engineering, Sichuan University, Chengdu 610065, China. (Yao Jin)

Graphical Abstract

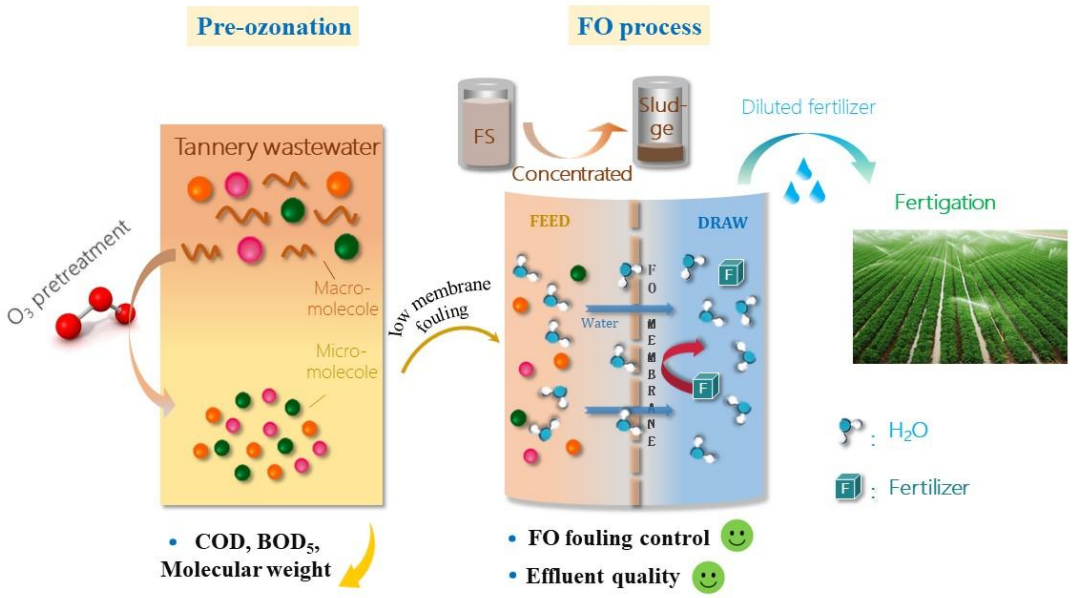

Abstract

Membrane-based processes have emerged as effective solutions for treating tannery wastewater. persistent membrane fouling remains a significant obstacle to long-term operational sustainability, and residual pollutants often persist in the treated effluent. To address these challenges, we investigated an integrated ozone - forward osmosis (O_3-FO) process, with a focus on evaluating the efficacy of pre-ozonation in alleviating membrane fouling, as well as exploring the possibilities of this integrated process for the reuse of tannery wastewater. Fertilizer, specifically 2 M $Ca(NO_3)_2$, served as the draw solution (DS) in this process. The findings reveal that the integrated system demonstrated remarkable pollutant retention capabilities. Notably, no metal was detected in the fertilizer. Therefore, the integrated process not only dilutes the fertilizer but also minimizes the risk of heavy metal contamination to both crops and soil. Furthermore, pre-ozonation effectively mitigated membrane fouling, resulting in an increase in membrane flux with a maximum increase of 20.98% at 0.6 L/min. Orthogonal partial least squares-discriminant analysis (OPLS-DA) revealed pre-ozonation has the most significant impact on four parameters: water flux (J_w), chemical oxygen demand (COD), fouling resistance (R_f) and oxidation reduction potential (ORP). Meanwhile, Ammonium nitrogen (NH_4-N) variation, dissolved organic carbon (DOC) variation and ORP played an important role in the four systems. Multi-criteria decision analysis (MCDA) showed that the 0.2 L/min O_3-FO system achieved the highest score (0.66), followed by 0.6 L/min (0.53), 0.4 L/min (0.41) and 0 L/min (0.29). This research offers a theoretical framework for the synergistic integration of advanced oxidation and membrane technology in the treatment of industrial wastewater.

Keywords: tannery wastewater; ozone; membrane fouling; forward osmosis; fertilizer.

1. Introduction

In the pursuit of carbon neutrality and the circular economy, the reuse of industrial wastewater has been increasingly emphasized. The tannery industry, one of the most polluting industries, consumes an average of 25 to 80 m^3 water to process one ton of raw materials, generating a considerable volume of wastewater [1]. The wastewater contains high concentrations of hide trimmings, chemicals, dissolved organic matter, and other substances due to the chemicals and organic materials used in the process [2–4]. This poses a substantial risk to ecosystems, human health and wildlife [5,6]. Therefore, the treatment and reuse of tannery wastewater are paramount.

Among the numerous treatment methods available, membrane technology stands out as a promising and effective approach due to its adaptability, excellent effluent quality, and desalination capabilities. In recent years, FO has garnered significant attention as an emerging membrane process [7]. Distinguishing itself from pressure-driven membrane processes, FO leverages the osmotic pressure generated by concentration gradients across the membrane as the driving force for filtration. This technology offers numerous advantages, including reduced membrane fouling, lower energy consumption, and high pollutant retention [8]. Typically, FO is employed to concentrate wastewater pollutants to higher levels, facilitating more efficient subsequent treatment process and/or the recovery of resources [9]. However, direct application of FO membranes to wastewater treatment can result in extremely high filtration resistance, leading to a significant reduction in water flux and the need for frequent cleaning. These limitations can shorten membrane lifespan, increase operational costs, and compromise treatment effectiveness [10,11]. Therefore, the development of effective pretreatment techniques is crucial for enhancing the performance and sustainability of FO in tannery wastewater treatment.

It has been demonstrated that pre-ozonation treatment has been effectively employed to mitigate membrane fouling in the treatment of diverse wastewater types [12–17]. However, there remains a gap in research exploring the application of pre-ozonation in reducing membrane fouling specifically in the treatment of tannery wastewater. Some

prior studies have shown that pre-ozonation is efficient in alleviating UF membrane fouling when treating simulated drinking water and domestic wastewater [13,18]. Conversely, another study did not observe a significant reduction of nanofiltration / reverse osmosis (NF/RO) membrane fouling through pre-ozonation treatment in the treatment of landfill leachate [16]. This discrepancy could be attributed to variations in ozone dose, wastewater characteristics, membrane type and operating conditions [16,19,20]. It is noteworthy that the pre-ozonation process can contribute to reducing the operational and maintenance costs of subsequent membrane processes [21].

Although the FO process represents an advanced system, the re-concentration of diluted DS remains a critical challenge. There are several treatment technologies available for DS regeneration, including electrodialysis [22], membrane distillation [23] and reverse osmosis [24], However, these processes are energy-intensive, adding complexity to the overall treatment system [25]. Some studies have explored the use of fertilizer as DS, where the fertilizer solution undergoes continuous dilution during the operational process. Subsequently, this diluted DS can be utilized for agricultural irrigation fertilization after filtration [26–28], This approach eliminates the need for additional water resources to dissolve and dilute the fertilizer. In the FO process, wastewater and fertilizer serve as feed and draw solutions, respectively. This method offers a viable solution for both wastewater treatment and water recovery for agricultural use, addressing DS re-concentration energy constraints and water resource scarcity. Additionally, the FO process can be utilized for seawater desalination, and its characteristics and differences compared to fertilizer irrigation are summarized in Table SM1. It can be observed that the use of the FO process for fertilizer irrigation is superior to that for seawater desalination.

Based on our current understanding, there has been no prior investigation into the extraction of irrigation water from tannery wastewater via FO treatment. Furthermore, the utilization of the combined pre-ozonation-FO process for treating tannery wastewater remains unreported, thus it is extremely interesting to study. Given the diverse characteristics of the wastewater, it is imperative to systematically assess the feasibility of this combined process. Recently, the introduction and employed of techniques, including orthogonal partial least squares-discriminant analysis (OPLS-DA) and multi-criteria

decision analysis (MCDA), have taken place [29–31]. These methodologies enable the most appropriate decisions by comprehensively considering multiple factors simultaneously [30,32]. In our study, OPLS-DA autonomously identifies and selects physicochemical indicators that significantly affect the wastewater treatment effect through a data-driven approach, enhancing the model's interpretability and predictive accuracy. Its S-plots provide intuitive visualization tools, helping us understand the impact of different O_3-FO systems on the wastewater treatment effect. At the same time, MCDA provides a comprehensive evaluation method by integrating multiple evaluation criteria. Its system scoring helps us quickly identify the optimal O_3-FO system, offering us a more comprehensive perspective. The combination of OPLS-DA and MCDA provides a complementary analytical method. OPLS-DA focuses on data-driven feature selection and prediction, while MCDA focuses on multi-criteria decision support. Key physicochemical indicators identified by OPLS-DA can be part of the MCDA evaluation criteria, thereby enhancing the scientific and accuracy of decision-making.

Therefore, we aimed to investigate the ability of the different O_3-FO systems in treating tannery wastewater and to identify the most suitable system in this work. Initially, the performance of the different O_3-FO systems for treating tannery wastewater was evaluated, encompassing the variation in pollutants and the FO membrane flux. Additionally, the influence of different O_3-FO systems on both the resistance to membrane fouling and the characteristics of membrane fouling were further examined. Subsequently, drawing from the experimental data, we utilized OPLS-DA to evaluate the extent to which diverse performance factors contribute to the overall variance within the system. MCDA was employed to analyze the different system scores, enabling us to derive the optimal O_3-FO system, which provides theoretical guidance for plant application.

2. Experimental Materials and Methodologies

2.1. Experimental configurations and methodologies

The tannery wastewater, originating from the chrome tanning section, was procured

from the National Engineering Laboratory for Clean Technology of Leather Manufacture situated in Sichuan Province, China. This effluent was stored under controlled conditions at 4℃. The comprehensive water quality parameters are outlined in **Table 1**. Prior to commencing each experiment, samples were thoroughly shaken, and all experiments were executed in batch mode, with multiple duplications to ensure accuracy. The experimental configurations encompassed a pre-ozonation process and a cross-flow forward osmosis unit, as schematically depicted in **Fig. 1**.

Table 1 Characteristics of the tannery wastewater

Parameters	value
pH	3.92 ± 0.01
ORP (mv)	195.08 ± 1.22
TDS (mg/L)	7.25 ± 0.07
Conductivity (mS/cm)	13.0 ± 0.7
Turbidity (NTU)	129.0 ± 0.2
Total phosphorus (mg/L)	203 ± 12
NH_4-N (mg/L)	24.35 ± 0.35
COD (mg/L)	3715 ± 21
DOC (mg/L)	1468.56 ± 7.16
Total Fe (mg/L)	1.13 ± 0.03
Total Cr (mg/L)	567 ± 6

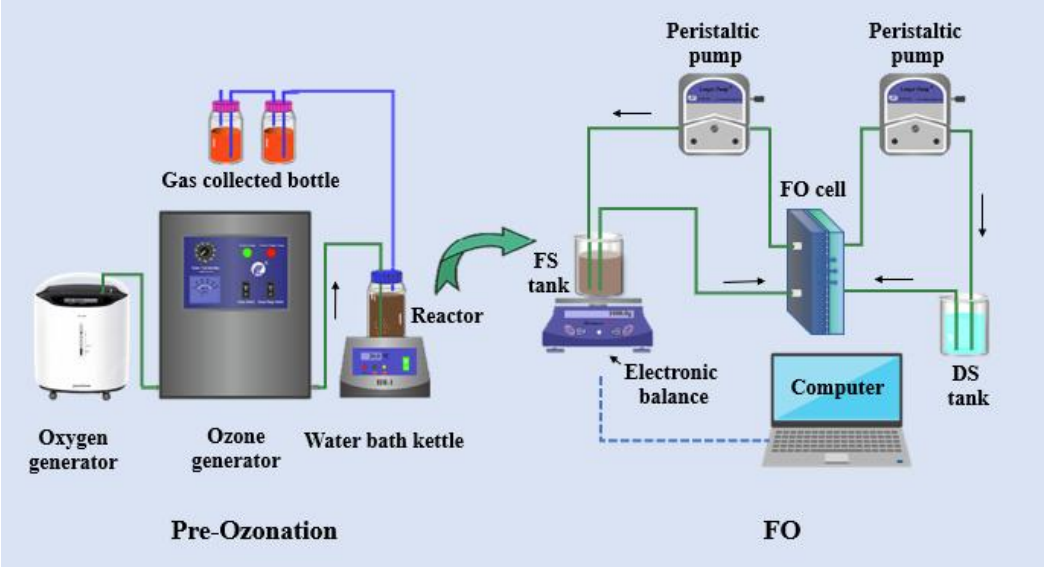

Fig. 1. Schematic diagram of the O_3-FO system.

During the pre-ozonation process, 800 ml of tannery wastewater was dispensed into 1 L glass bottles. A water bath (HH-1A, Beijing Kewei Yongxing Instrument Company, China) maintained the temperature at 20 ± 1°C, ensuring stability throughout the experiment. Ozone, generated from 90% oxygen (v/v), was injected at desired flow rates through a gas diffuser positioned at the bottom. The pre-ozonation reaction duration was standardized at 60 minutes, with an inlet ozone concentration of 54 ± 2 mg/L, supplied by the ozone generator (Beijing Tonglin Co., Ltd., China). To eliminate residual ozone, glass bottles containing KI solution were placed at the conclusion of the pre-ozonation process. Drawing from prior research on wastewater treatment using ozone [33–36], three different ozone flow rates (0.2, 0.4, and 0.6 L/min) were employed to treat the tannery wastewater, followed by membrane filtration.

In this research, a flat-sheet cellulose triacetate–polyester (CTA-ES) forward osmosis membrane was utilized, procured from Hydration Technology Innovations (HTI), located in Albany, California, USA. This membrane is a quintessential asymmetric CTA-ES type,

191 featuring a thin active layer made of cellulose triacetate and a robust polyester mesh
192 support layer, which respectively offer selectivity and mechanical support for the
193 membrane. The fundamental specifications of the membrane are detailed as follows: the
194 rejection rate for sodium chloride is 97%; the membrane substance is composed of CTA;
195 it operates effectively within a pH range of 3 to 8; the operational temperature is from 5
196 to 60°C; and the water permeability coefficient is recorded at 0.98 L/(m²h·bar) [37]. The
197 cross-flow FO system boasted an efficient membrane area measuring 33.15 cm^2 and
198 functioned in the active layer facing feed solution (ALFS) mode. For the FO experiment,
199 calcium nitrate ($Ca(NO_3)_2$) was chosen as the draw solution due to its comparably low
200 reverse solute flux (RSF) in comparison to other fertilizers. Additionally, 2M $Ca(NO_3)_2$
201 can effectively generate the required osmotic pressure during the FO process [26]. A
202 volume of 500 ml of the O_3 treatment solution served as the feed solution, while 500 ml
203 of 2 M $Ca(NO_3)_2$ acted as the draw solution, which provides an initial osmotic pressure of
204 108.5 atm [26]. These solutions were continuously circulated through the membrane cell
205 and returned to the respective tanks, maintained at a shear rate of 6.4 $m \cdot s^{-1}$ for a duration
206 of 8 hours, facilitated by two peristaltic pumps (BT600S, Lead Fluid Technology Co.,
207 Ltd., China).
208 Prior to its utilization, the FO membrane underwent a purification process, involving
209 immersion in ultrapure water for 24 hours to eliminate impurities and additives leftover
210 from the manufacturing process. The electronic balance accurately measured the mass of
211 the FO feed solution, and a computer recorded the data in time for the subsequent
212 calculation of membrane flux. Once the filtering operation was completed, the FO
213 membranes were dried at a temperature of 40°C, in preparation for membrane surface
214 study.

215 *2.2. Membrane flux and fouling resistance evaluation*

216 The fouling resistance (R_f) was determined as follows:

217 $$R_f = \frac{\Delta\pi}{\mu \cdot J} \quad (1)$$

218 where the unit of R_f is m^{-1}, $\Delta\pi$ represents the transmembrane pressure difference
219 caused by fertilizer (pa), μ signifies the viscosity of the water at 25°C (pa·s) and J is

the permeate flux ($m^3 \cdot m^{-2} \cdot s$).

Additionally, the model of membrane fouling tendency was utilized to evaluate the rate of fouling accumulation in the FO membrane. By fitting the filtration time and permeate volume data of FO membrane, the fouling coefficient K_0 of the FO membrane after pre-ozonation treatment could be calculated as follows:

$$V = \frac{A}{K_0} \ln\left(\frac{K_0 \Delta\pi}{\mu R_m} t + 1\right) \quad (2)$$

where R_m, V, A, t stand for the intrinsic membrane resistance (m^{-1}), filtrate volume (m^3), effective membrane area (m^2) and filter time (h), respectively [38].

2.3. OPLS-DA and MCDA

In this work, OPLS-DA was employed to assess the impact of diverse system performance factors on the overall system variance. The analysis, including model cross-validation and variable importance in projection (VIP), was executed utilizing the SIMCA 14.1 software (Umetrics, Umeå, Sweden). Additionally, the Multi-Criteria Decision Analysis (MCDA) framework was utilized to determine the criterion weights and scores for different O_3-FO systems in order to derive the best O_3-FO system, aiming to identify the optimal system for practical applications. The dataset encompassed seven variables, including water flux, oxidation-reduction potential (of the FO draw solution), conductivity (of the wastewater after pre-ozonation), fouling resistance, NH_4–N variation, DOC variation and COD variation, pertaining to the O_3-FO system.

Within the MCDA framework, the Technique for Order Preference by Similarity to Ideal Solution (TOPSIS) method was utilized for computing the weights and scores of the different O_3-FO systems, leveraging the Matlab program (MathWorks, Inc., USA). Briefly, a seven-step process was followed to compute the scores [29]. Initially, a matrix (M) was constructed, encompassing four systems and seven criteria. The matrix was standardized through the application of the vector normalization technique, leading to the creation of a uniformly scaled decision matrix, designated as (D). Subsequently, the matrix (D) was scaled further by incorporating the specific weight assigned to each individual parameter, thus yielding a weighted normalization matrix (N). For each system, both positive and negative ideal reference points were identified. These reference points

were then leveraged to compute scores across the entire spectrum of systems, providing a comprehensive evaluation. These scores served as indicators of the appropriateness level for each O_3-FO system. **Fig. 2** provides a visual representation of the calculation process.

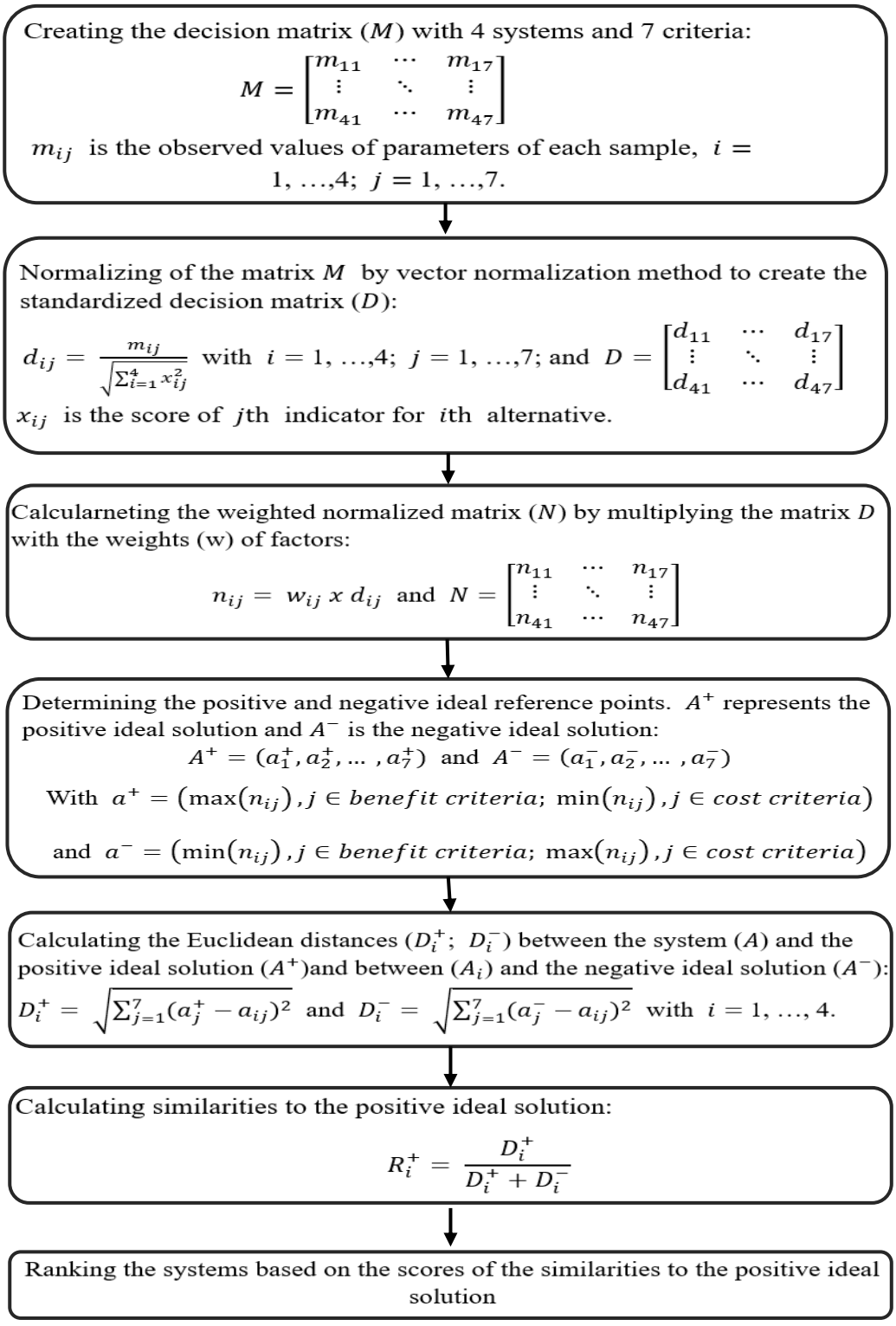

Fig. 2. The MCDA protocol for constructing O_3-FO systems index.

2.4. Analytical techniques

The biochemical oxygen demand (BOD), COD, DOC, and turbidity values were measured using a biochemical incubator (LRH-250, Yiheng, Shanghai, China), a COD detector (COD-571, Leici, Shanghai, China), an automatic carbon and nitrogen analyzer (Vario TOC, Elementar, Germany) and a turbidity meter (WZS-186, Leici, Shanghai, China), respectively. Additionally, conductivity, pH, total dissolved solids (TDS), ORP were determined utilizing a multi-parameter analyzer (DZS-708-A, Leici, China) [38]. NH_4-N and total phosphorus (TP) concentrations were determined using a water quality tester (DRB 200, HACH, Shanghai, China). The viscosity was measured using a rotational rheometer (Anton Paar, MCR 302). The instrument was equipped with a CP50-1 cone (diameter 50 mm, angle 1°). During the measurement process, the shear rate was gradually increased from 0.1 s^{-1} to 300 s^{-1}, and the viscosity was determined at a shear rate of 300 s^{-1}. The viscosity values at the flow rates of 0, 0.2, 0.4, and 0.6 L/min were 1.575×10^{-3}, 1.398×10^{-3}, 1.301×10^{-3}, and 1.237×10^{-3} Pa·s, respectively.

To gain insights into membrane surface morphology and elemental compositions, scanning electron microscopy (SEM) (Apreo S, Thermo Fisher Scientific, US) augmented with energy dispersive spectroscopy (EDS) (Aztec X-Max80, Oxford-Instruments, UK) was employed. Additionally, inductively coupled plasma emission spectrometer (ICP-OES) (Optima8000, PerkinElmer, US) was utilized to analyze the iron (Fe) and chromium (Cr) ion content of tannery wastewater [39].

For characterizing the types of dissolved organic matter present in tannery wastewater following treatment with different ozone flow rates, a fluorescence spectrophotometer (F-7000, Hitachi, Japan) was used. The excitation wavelengths ranged from 200 to 400 nm with a sampling interval of 5.0 nm, while the emission range extended to longer wavelengths from 250 to 500 nm, with a step size of 1 nm for each excitation wavelength.

3. Analysis and interpretation of results

3.1. Efficiency of O_3-FO process

3.1.1. Pollutants Variation

The effluent quality for different ozone flow rates and FO draw solutions is depicted in **Fig. 3** (Details are presented in Table SM2 and Table SM3). During the pre-ozonation process, a gradual decrease in COD and TP contents was observed with increasing ozone flow rates, indicating the degradative effect of ozone on organic matter and organophosphorus. However, it is noteworthy that the maximum degradation rates for COD and TP were 18.7% and 63.8% (at 0.6 L/min), respectively, revealing a relatively low COD degradation rate. The relatively low COD degradation rates align with previous reports [34,35]. Notably, pre-ozonation had minimal impact on the content of NH_4-N, Fe, Cr.

After being treated with FO membrane, the concentrations of all pollutants were significantly reduced and the retention efficiencies of the FO membrane for COD, DOC and NH_4-N were 80-90.4%, 94.7-95.7% and 49.8-59.1% respectively. Moreover, Fe, Cr, and TP were undetectable in the draw solution, which indicates the significant retention efficiency of the FO unit for metals and phosphorus.

In summary, the integrated O_3-FO system demonstrates excellent removal and retention capabilities for pollutants. It is worth noting that the fertilizer concentration in the effluent is relatively high and requires appropriate slight dilution before use. Afterward, the effluent from the O_3-FO process can meet the irrigation standards (Table SM4).

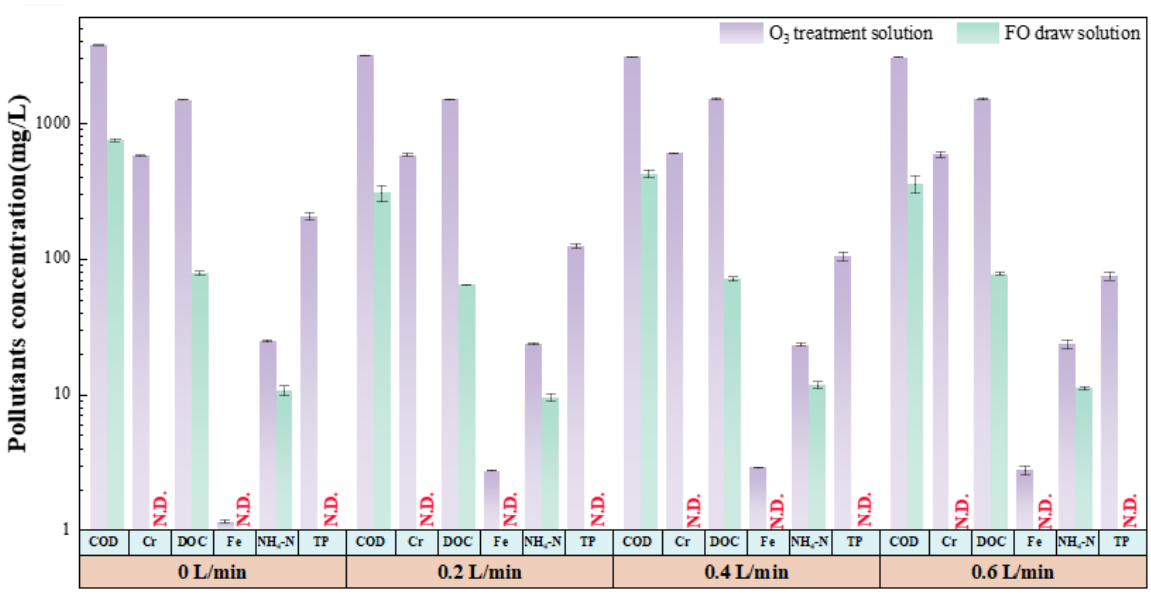

303

304 **Fig. 3.** The effluent quality of different ozone flow rates (0-0.6 L/min) and FO draw
305 solutions. All units are in mg/L. "N.D." denotes no decision.

306 *3.1.2. Removal of organics*

307 The graphical representation of the changes in UV absorbance at 254 nm (UV_{254}),
308 DOC and specific UV absorbance (SUVA) at various ozone flow rates is presented in **Fig.**
309 **4**a. It is evident that as the flow rate of ozone increases, the UV_{254} value decreases,
310 indicating a reduction in the molecular weight of the organic pollutants. the initial rise in
311 DOC contents was followed by a decrease as the ozone flow rate increased. This trend
312 could be explained by the dissolution of emulsifiers and degreasing agents, and other
313 macromolecular organics present in the raw tannery wastewater at lower ozone flow rates
314 (0.2 and 0.4 L/min), followed by their degradation at higher rates (0.6 L/min). Another
315 possibility is that ozonation of microbial structures led to the release of intracellular
316 substances[40,41]. This phenomenon is consistent with findings from another study [36].
317 The SUVA, calculated as the ratio of UV_{254} to DOC, is an indicator of the aromaticity
318 of the dissolved organic matter in tannery wastewater. As the ozone flow rate increases,
319 the SUVA value, which was initially 0.177 $L \cdot mg^{-1} \cdot m^{-1}$ in the raw water, decreases to
320 0.160, 0.150, and finally to 0.146 $L \cdot mg^{-1} \cdot m^{-1}$. The SUVA value remains below 2
321 $L \cdot mg^{-1} \cdot m^{-1}$, suggesting that the organic components in the wastewater are predominantly
322 of low hydrophobicity and low molecular weight [42].

Fig. 4b illustrates that the BOD_5/COD ratio increases from 0.28 in the raw wastewater to 0.31 after pre-ozonation, indicating that pre-ozonation can enhance the biodegradability of tannery wastewater. This improvement is likely due to the transformation of complex organic compounds into simpler, more biodegradable forms [43,44]. However, it should be noted that the effectiveness of ozone in enhancing biodegradability is not as significant as the improvements reported with the use of catalysts in other studies [34].

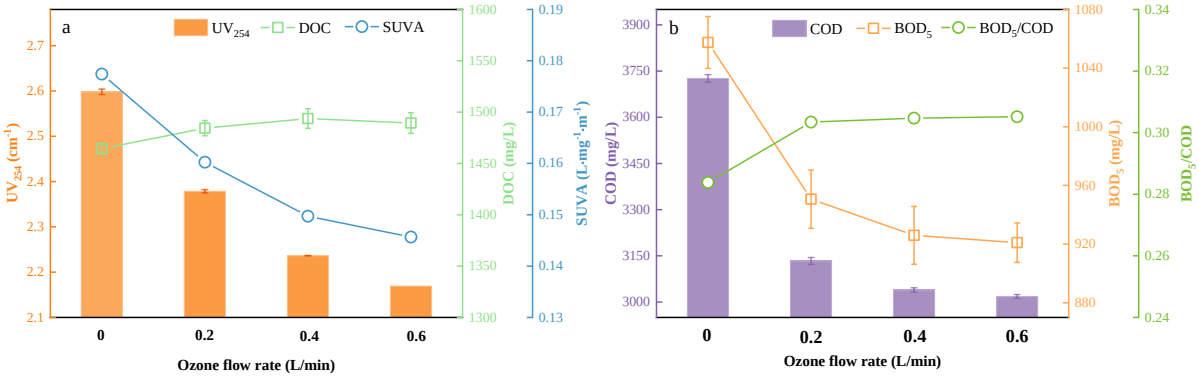

Fig. 4. The impact of pre-ozonation on organic parameters.

The experimental data were linearly fitted using a pseudo-first-order kinetic equation to obtain the degradation rate constants of ozone for COD, DOC, and TP. The fitting curve equation is displayed in Table SM5. **Fig. 5**a shows that the degradation rate of ozone for TP (0.467 min^{-1}) is significantly higher than that for COD (0.092 min^{-1}) and DOC (0.094 min^{-1}), indicating that ozone exhibits competitive degradation for different pollutants, which may be the reason for the low removal rates of COD and DOC by pre-ozonation. At the same time, it was found that the degradation rate of pollutants would be reduced with prolonged ozone treatment time (**Fig. 5**b). This finding suggests that relying solely on ozone treatment is inappropriate, underscoring the need to couple ozone with other processes.

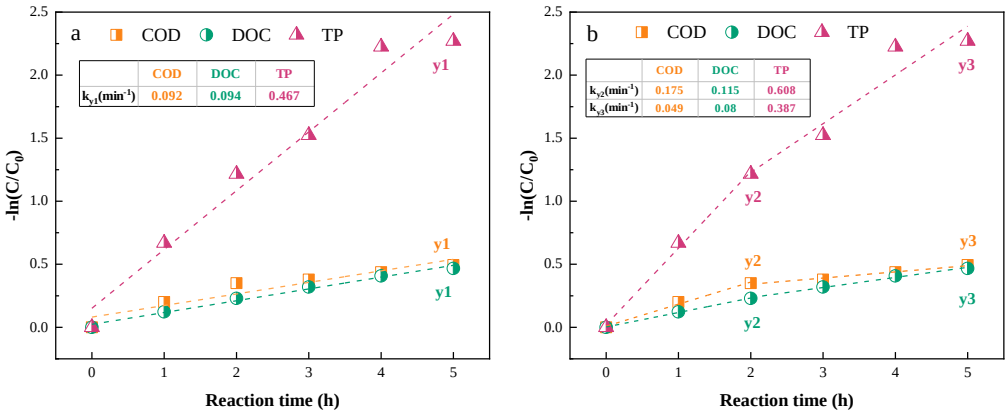

Fig. 5. Pseudo-primary degradation diagram of COD, DOC and TP in tannery wastewater treated with 0.2 L/min O_3.

3.1.3. Variation of dissolved organic matter

The investigation into the fluctuation of dissolved organic matter in tannery wastewater across different ozone flow rates was conducted through the acquisition of 3D fluorescence spectra. The fluorescence region integration technique was utilized to categorize the EEM spectrum into five distinct regions: Region I, characterized by Ex/Em wavelengths of 220-250/280-330 nm, representing aromatic proteins; Region II, with Ex/Em wavelengths of 220-250/330-380 nm, also pertaining to aromatic proteins; Region III, covering Ex/Em wavelengths of 220-250/380-540 nm, indicative of fulvic acid species; Region IV, defined by Ex/Em wavelengths of 250-440/280-380 nm, corresponding to soluble microbial by-products and finally, Region V, with Ex/Em wavelengths of 250-400/380-540 nm, representing humic acid-like substances [45]. The fluorescence regional integration (FRI) is used for semi-quantitative analysis of dissolved organic matter (DOM) in tannery wastewater.

Fig. 6(a-d) illustrates that fulvic acid-like substances and humic acid-like components constitute the primary organic constituents in the raw tannery wastewater, which were more than aromatic proteins and soluble microbial by-product-like substances. As the ozone flow rate (0.2, 0.4 L/min) increased, the fluorescence intensity of organic matter

increased, especially for region III, region IV, and region V. The fluorescence intensity of these three regions decreased at 0.6 L/min (**Fig. 6**e), which is probably attributed to undissolved emulsifiers, degreasing agents and other macromolecular organics in the raw tannery wastewater were dissolved at low ozone flow rates (0.2, 0.4 L/min) and degraded at high ozone flow rates (0.6 L/min). This phenomenon is closely related to the variation of DOC values.

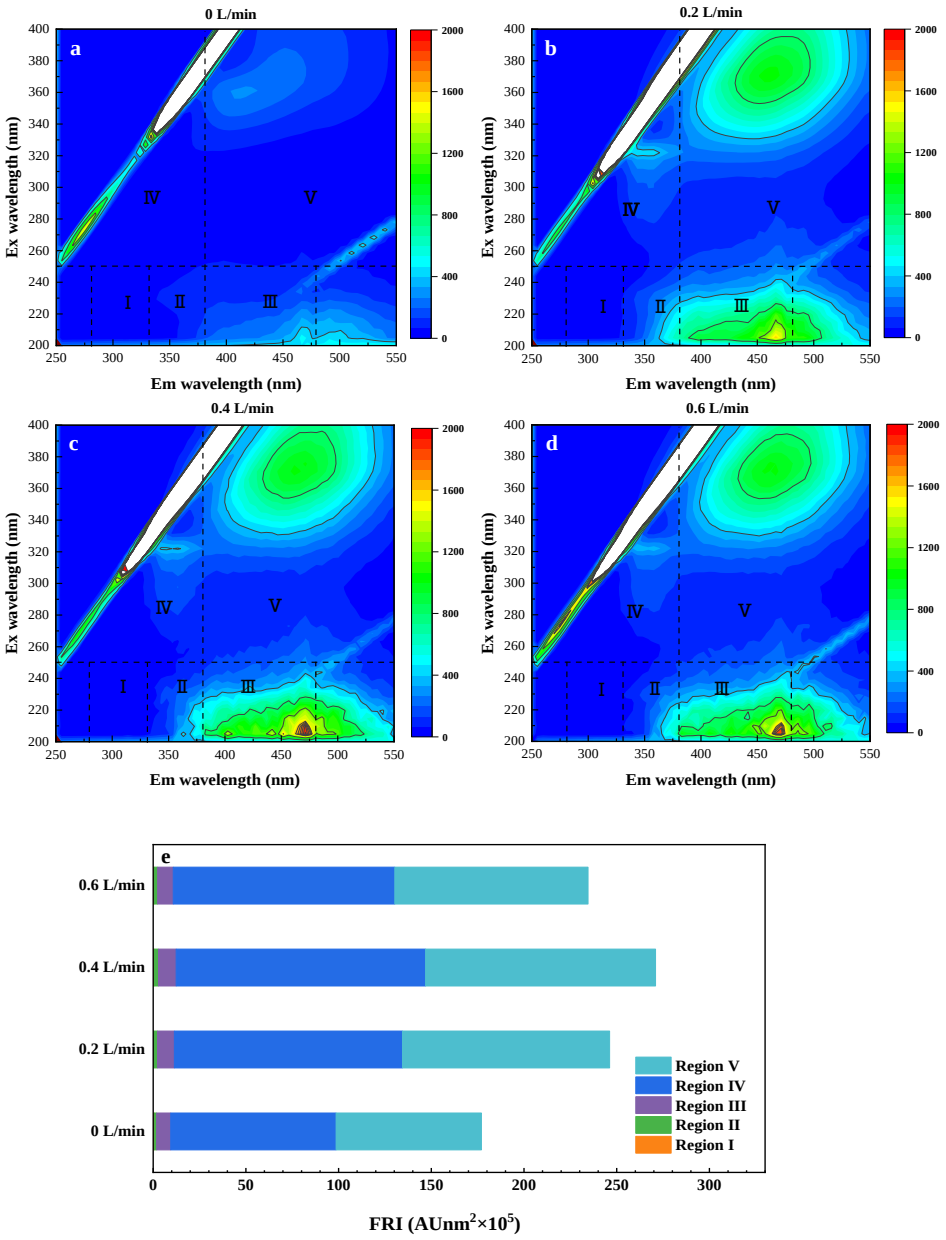

Fig. 6. 3D EEM fluorescence spectra of treatment solutions with different O_3 flow rates: (a) 0 L/min; (b) 0.2 L/min; (c) 0.4 L/min; (d) 0.6 L/min. (e) FRI distribution of treatment solutions with different O_3 flow rates.

The EEM fluorescence spectra of FO draw solutions are presented in **Fig. 7**(a-d). Compared to **Fig. 6**, it is observed that the dissolved organic matter in the DS is considerably less than that found in the O_3 treatment solution, as indicated by the scale.

This observation underscores the remarkable retention efficiency of the FO membrane in filtering out dissolved organic matter, which aligns with its performance in retaining DOC. Furthermore, as the O_3 flow rate increases, a gradual augmentation in the fluorescence intensity of the FO draw solution is observed. This phenomenon can be attributed to the enhanced membrane flux at higher ozone flow rates, leading to a greater permeability of dissolved organic matter into the draw solution. The FO membrane flux is discussed in section 3.2.1.

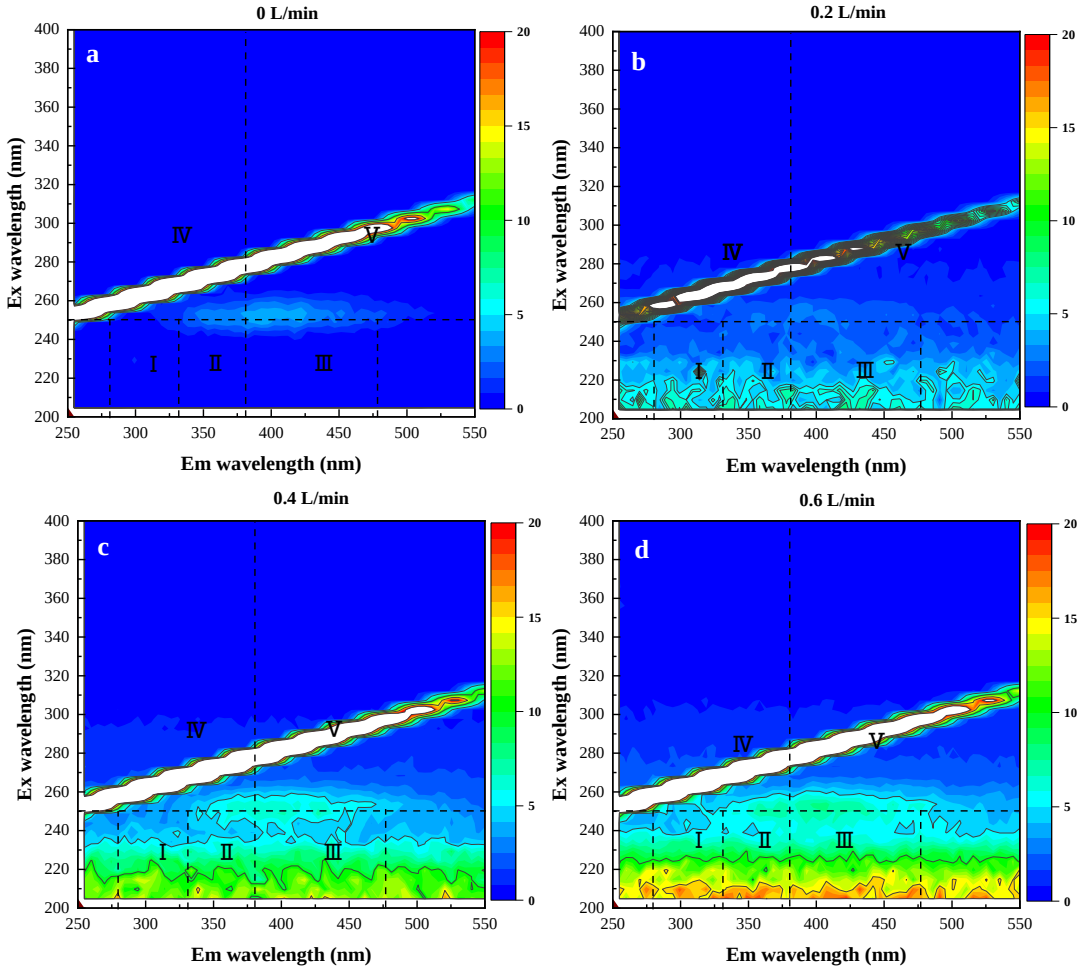

Fig. 7. 3D EEM fluorescence spectra of FO draw solutions.

3.2. FO membrane performance

3.2.1. Performance evaluation of water flux and membrane fouling

Fig. 8a depicts the FO membrane fluxes at different ozone flow rates and it was found

that the membrane fluxes increased gradually with increasing O_3 flow rate. In the final stage of the experiment, the membrane flux continued to maintain a high level at the higher ozone flow rates. In addition, membrane fouling resistance gradually decreased with increasing ozone flow rate (**Fig. 8**b). This finding, coupled with the observed impact of pre-ozonation on pollutants, suggests that pre-ozonation effectively degrades contaminants in tannery wastewater, thereby mitigating membrane fouling and enhancing membrane flux. This establishes a theoretical foundation for the effective treatment of tannery wastewater in industrial applications.

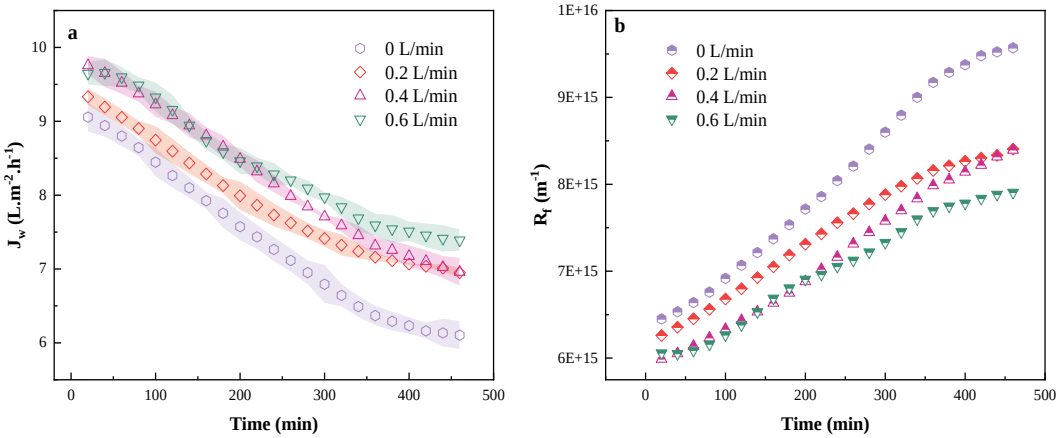

Fig. 8. Variation of FO membrane flux (a) and fouling resistance (b) under different flow rates of ozone.

By fitting the experimental data from the FO membrane filtration, the fouling tendency coefficient K_0 can be obtained. The fitting process was illustrated in **Fig. 9**(a-d), where it was observed that the correlation coefficients R^2, calculated for data fitting under four different ozone flow rates, were all greater than 0.98, indicating a high correlation between the mechanistic model and the filtration data. As shown in **Fig. 9**e, the K_0 value gradually decreases with the ozone flow rate increases, suggesting that the rate of fouling accumulation on the FO membrane decreases progressively as the ozone flow rate increases. This further demonstrates that pre-ozonation can effectively reduce FO

membrane fouling.

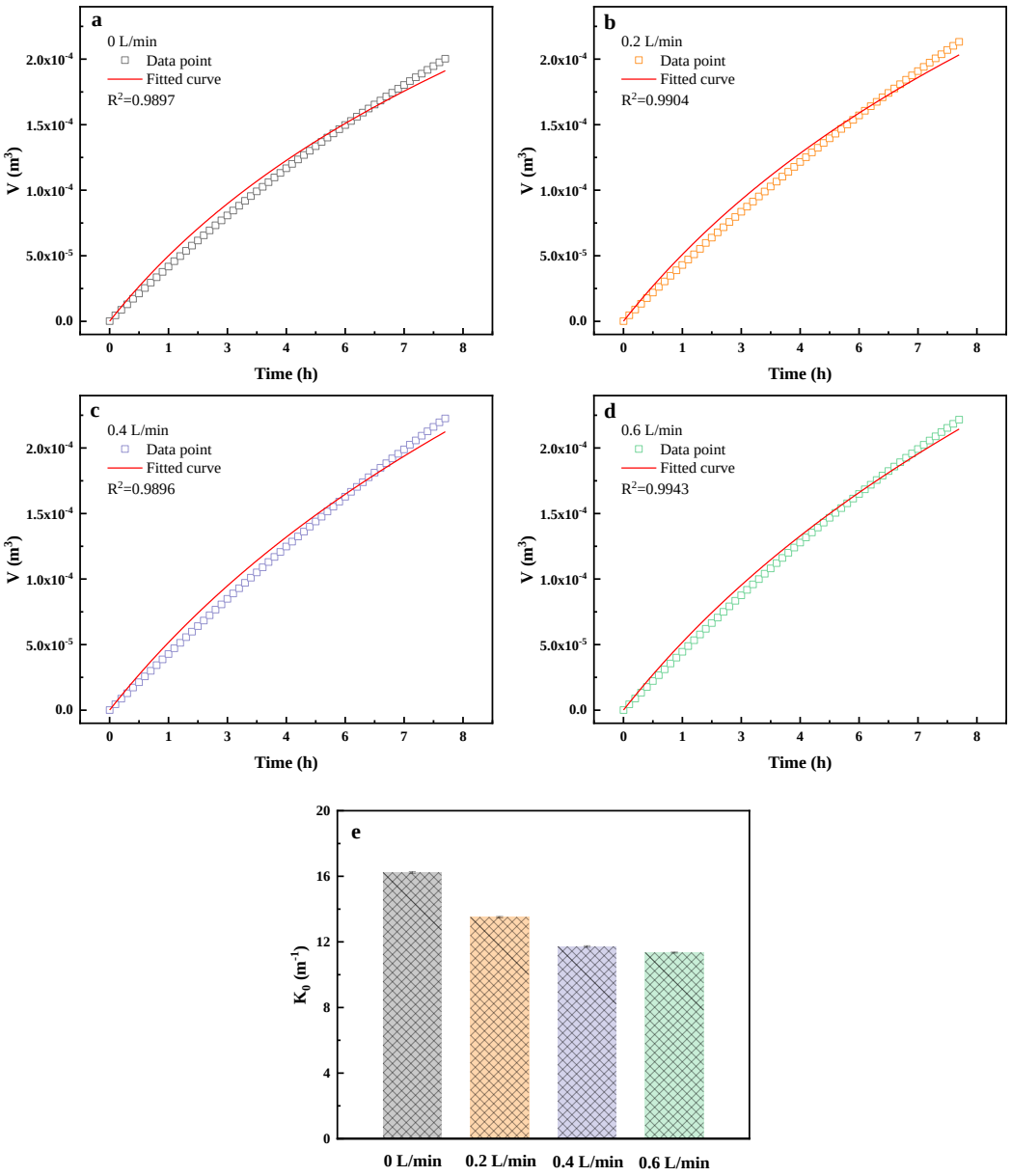

Fig. 9. K_0 fitting graph and K_0 value of FO filtration data at different ozone flow rates.

3.2.2. Characteristics of the fouling layer on the FO membrane surface

The impact of different ozone flow rates on the fouling of FO membranes was characterized through the examination of the membrane's surface morphology and the

elemental composition of the cake layer, utilizing SEM and EDS measurements respectively (**Fig. 10**). By SEM analysis, observations revealed that the particles present on the cake layer's surface were exposed under pre-ozonation, indicating that the pollutants in the tannery wastewater were degraded or removed under pre-ozonation leading to some crystal particles not being encapsulated. Furthermore, EDS analysis revealed that the cake layer on the FO membrane comprised primarily of C, N, O, Cr, S, Na, Cl, Ca and Fe, suggesting that both organic and inorganic materials contributed to the FO membrane fouling. With an increase in the ozone flow rate, the percentage of C element in the cake layer decreased, from 40.91% to 27.78%, 30.96% and 20.21%. indicating that the organic matter in the tannery wastewater was removed or degraded to small organic molecules by pre-ozonation.

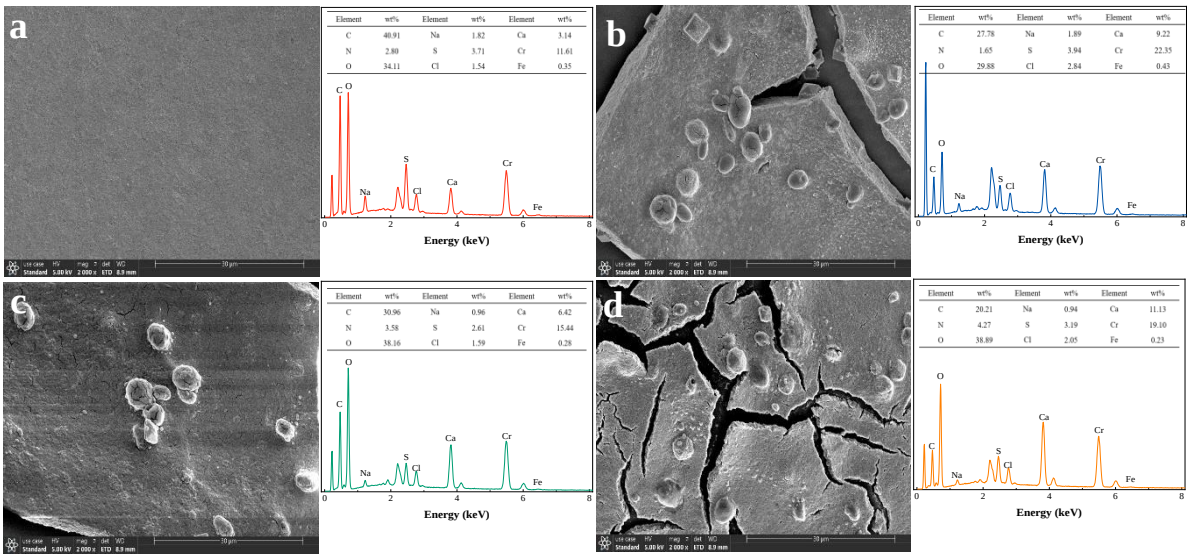

Fig. 10. Analyses of surface morphology and elemental composition of UF membrane cake layers at different ozone flow rates: (a) 0 L/min; (b) 0.2 L/min; (c) 0.4 L/min; (d) 0.6 L/min. The EDS plots provided the respective weight percentages of the elements. All surface images were magnified at 2000×.

3.3. Assessing the individual contributions of indicators towards the overall variance of the O_3-FO system

To assess the relative contribution of various indicators to the overall variance within the O_3-FO system, the OPLS-DA was performed on the dataset collected in this

investigation. The details of the dataset are provided in Table SM6. The results of the OPLS-DA are presented in **Fig. 11**a, where A, B, C and D represent 0 L/min, 0.2 L/min, 0.4 L/min and 0.6 L/min O_3-FO systems respectively. It could be observed that the parallel samples of each system were closer together, indicating minimal variability among the samples. Upon further analysis of **Fig. 11**a, we observe significant differences in the physicochemical indicators between the ozone flow rate of 0 L/min and the other three systems (i.e., systems with ozone flow rates), indicating that the physicochemical indicators of tannery wastewater are greatly affected under ozonation treatment. However, once the ozone flow rate is introduced and increased, we notice that the differences between systems under various ozone flow rates gradually diminish. This may imply that once ozonation treatment is initiated, the further improvement effect of increasing the flow rate on the physicochemical indicators is limited, suggesting the existence of an optimal ozone flow rate point. Beyond this point, the contribution of increasing the ozone flow rate to enhancing the wastewater treatment effect decreases.

During this evaluation, the independent variable fit index (R_x^2) attained a value of 0.985, the dependent variable fit index (R_y^2) registered a score of 0.933 and the model prediction index (Q^2) was measured as 0.874. Theoretically, it is preferable for R^2 and Q^2 values to be close to 1. In general, values of R^2 and Q^2 exceeding 0.5 are considered satisfactory, while values above 0.4 are still acceptable[31].

Following 200 permutation tests, as depicted in **Fig. 11**b, the intersection of the Q^2 regression line with the vertical axis was fell below 0, signifying the absence of overfitting in the model. This confirms the reliability of the model and ensures the confident utilization of its results for performance analysis across different systems. VIP scores were employed to assess the importance of the indicator in distinguishing differences between systems. An indicator was considered crucial in discriminating between systems when its VIP score exceeded 1. In this analysis, NH_4-N variation, DOC variation and ORP emerged as key indicators, playing a significant role across all four systems (**Fig. 11**c).

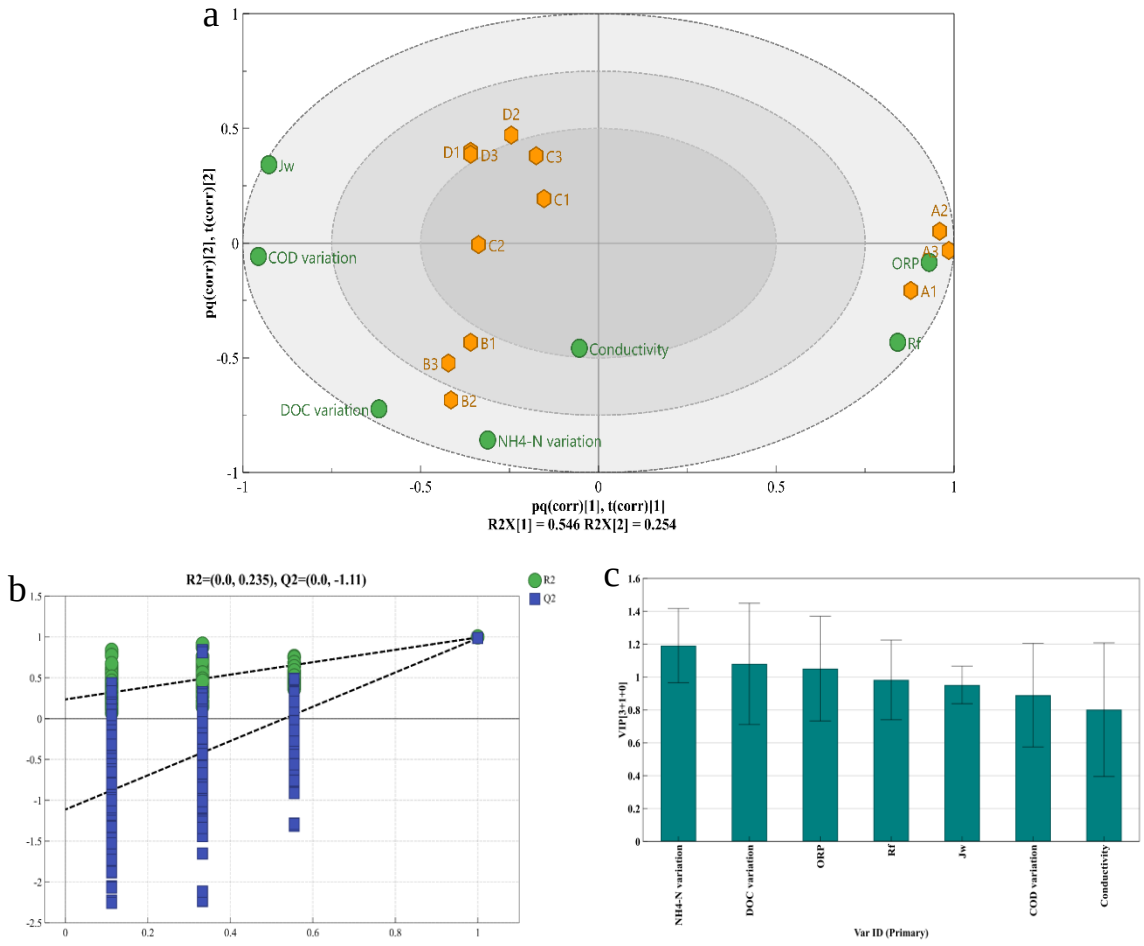

Fig. 11. (a) OPLS-DA, (b) the permutation test of OPLS-DA model and (c) variable importance in projection of different O_3-FO system.

3.4. Appropriateness evaluation of the different O_3-FO system

To comprehensively evaluate the various performance elements of the calculations, the influence of each factor (whether positive or negative) was determined through an understanding of how the indicators influence the overall functionality of the system. The statistical data sets for the performance of the different O_3-FO systems were also presented in the **Table 2**. It can be observed that the weight values of NH_4-N variation, DOC variation and ORP are significantly greater compared to other parameters, aligning with the results of OPLS-DA.

Utilizing the dataset in **Table 2**, the scores for the different O_3-FO systems were calculated adhering to the methodological part of the procedure shown in **Fig. 2**. During

this computation, the scores were determined by assessing the resemblance between the investigated O_3-FO system and the optimal state, with the highest attainable score being 1.

The scores and corresponding rankings of the different O_3-FO systems are summarized in **Table 3**. The 0.2 L/min O_3-FO system emerged as the top performer in all evaluated aspects, attaining a maximum score of 0.66, indicating the closest resemblance to the ideal state. Subsequently, the 0.6 L/min, 0.4 L/min, and 0 L/min systems followed suit. This signifies that the most suitable system is one that effectively balances various system performance aspects, a crucial consideration, especially in the prolonged operation of the system. Furthermore, the operational and maintenance costs of the ozonation process are approximately $0.65 - 0.72$ \$/m^3 [36]. Despite the potential for higher flow rates to improve membrane flux and pollutant removal efficiency, these enhancements are not notably significant. When taking economic considerations into account, a flow rate of 0.2 L/min emerges as the most economically viable option. Consequently, the 0.2 L/min O_3-FO system is distinguished as the optimal choice, balancing both performance and economic feasibility.

Table 2 Dataset pertaining to the multi-criteria decision analysis (MCDA).

Criteria	Water flux (J_w, $L \cdot m^{-2} \cdot h^{-1}$)	ORP (mv)	Conductivity ($\mu s \cdot cm^{-1}$)	Fouling resistance (R_f, m^{-1})	NH_4-N variation (mg/L)	DOC variation (mg/L)	COD variation (mg/L)
Weight	0.105	0.186	0.107	0.112	0.192	0.195	0.103
Influence	+	+	-	-	+	+	+
0 L/min O_3-FO	6.15 ± 0.01	302.83 ± 0.51	12.95 ± 0.69	9.79E+15 ± 4.01E+14	13.57 ± 0.60	1391.18 ± 2.27	2977 ± 83
0.2 L/min O_3-FO	7.02 ± 0.02	287.90 ± 0.30	13.74 ± 0.75	8.64E+15 ± 1.81E+14	15.20 ± 0.36	1405.09 ± 0.53	3413 ± 31
0.4 L/min O_3-FO	7.07 ± 0.04	284.27 ± 0.40	12.76 ± 1.61	8.41E+15 ± 9.89E+13	13.10 ± 0.50	1398.39 ± 2.10	3297 ± 88
0.6 L/min O_3-FO	7.44 ± 0.02	289.53 ± 0.72	12.43 ± 1.51	7.66E+15 ± 2.31E+14	13.57 ± 0.29	1392.46 ± 2.05	3363 ± 39

Table 3 The scores and rankings for each O_3-FO system

Types	The score index	Ranking
0 L/min O_3-FO	0.29	4
0.2 L/min O_3-FO	**0.66**	**1**
0.4 L/min O_3-FO	0.41	3
0.6 L/min O_3-FO	0.53	2

4. Conclusion

In this study, an integrated O_3-FO process was employed to evaluate the efficacy of pre-ozonation in alleviating membrane fouling and investigate its potential for reusing tannery wastewater. The main discoveries are summarized below:

- Pre-ozonation alone proved insufficient for the removal of pollutants, yet the FO membrane exhibited remarkable retention capabilities. Notably, the retention rates of COD, DOC and NH_4-N were 80-90.4%, 94.7-95.7% and 49.8-59.1% respectively. After appropriate slight dilution of the effluent from the integrated system, it can meet the irrigation standards.
- No Fe and Cr ions were detected in the DS. Therefore, the integrated process has the following advantages:

  a: Dilution of fertilizers.

  b: Minimizing the risk of heavy metal contamination to both crops and soil.
- Pre-ozonation effectively reduces membrane fouling, thereby enhancing membrane flux, with a maximum improvement of 20.98% achieved at 0.6 L/min. This phenomenon holds significant implications for industrial applications.
- OPLS-DA revealed pre-ozonation has the most significant impact on four parameters: J_w, COD variation, R_f, and ORP. Concurrently, NH_4-N variation, DOC variation and ORP played an important role in the four systems.
- MCDA indicated that the 0.2 L/min O_3-FO system emerged as the most effective, scoring the highest (0.66), followed by 0.6 L/min (0.53), 0.4 L/min (0.41) and 0 L/min (0.29).

Declaration of Competing Interest

The authors declare that they have no known competing financial interests or personal relationships that could have appeared to influence the work reported in this paper.

Data availability

Data will be made available on request

Acknowledgments

This work was sponsored by National Natural Science Foundation of China (Grant number: 21978175), Sichuan Science and Technology Program (Grant number: 2019YJ0109) and Fundamental Research Funds for the Central Universities of China (Grant number: YJ201835).

References

[1] E.M. Romero-Dondiz, J.E. Almazán, V.B. Rajal, E.F. Castro-Vidaurre, Removal of vegetable tannins to recover water in the leather industry by ultrafiltration polymeric membranes, Chem. Eng. Res. Des. 93 (2015) 727–735. https://doi.org/10.1016/j.cherd.2014.06.022.

[2] A. Cassano, R. Molinari, M. Romano, E. Drioli, Treatment of aqueous effluents of the leather industry by membrane processes: A review, J. Membr. Sci. 181 (2001) 111–126. https://doi.org/10.1016/S0376-7388(00)00399-9.

[3] J. Zhao, Q. Wu, Y. Tang, J. Zhou, H. Guo, Tannery wastewater treatment: conventional and promising processes, an updated 20-year review, J. Leather Sci. Eng. 4 (2022) 10. https://doi.org/10.1186/s42825-022-00082-7.

[4] C.R. China, R. Elibariki, J. Msami, S. Mwombela, L. Wilson, Technical and technological constraints facing Tanzania leather value chain: a snapshot of intervention measures, J.

Leather Sci. Eng. 4 (2022) 20. https://doi.org/10.1186/s42825-022-00095-2.

[5] A. Cassano, J. Adzet, R. Molinari, M.G. Buonomenna, J. Roig, E. Drioli, Membrane treatment by nanofiltration of exhausted vegetable tannin liquors from the leather industry, Water Res. 37 (2003) 2426–2434. https://doi.org/10.1016/S0043-1354(03)00016-2.

[6] F. Yang, X.-B. Wang, Y. Shan, C. Wu, R. Zhou, N. Hengl, F. Pignon, Y. Jin, Research recap of membrane technology for tannery wastewater treatment: a review, Collagen Leather 5 (2023) 24. https://doi.org/10.1186/s42825-023-00132-8.

[7] S. Kim, K.H. Chu, Y.A.J. Al-Hamadani, C.M. Park, M. Jang, D.-H. Kim, M. Yu, J. Heo, Y. Yoon, Removal of contaminants of emerging concern by membranes in water and wastewater: A review, Chem. Eng. J. 335 (2018) 896–914. https://doi.org/10.1016/j.cej.2017.11.044.

[8] A.J. Ansari, F.I. Hai, W.E. Price, J.E. Drewes, L.D. Nghiem, Forward osmosis as a platform for resource recovery from municipal wastewater - A critical assessment of the literature, J. Membr. Sci. 529 (2017) 195–206. https://doi.org/10.1016/j.memsci.2017.01.054.

[9] X. Wang, T. Hu, Z. Wang, X. Li, Y. Ren, Permeability recovery of fouled forward osmosis membranes by chemical cleaning during a long-term operation of anaerobic osmotic membrane bioreactors treating low-strength wastewater, Water Res. 123 (2017) 505–512. https://doi.org/10.1016/j.watres.2017.07.011.

[10] S.M. Riley, J.M.S. Oliveira, J. Regnery, T.Y. Cath, Hybrid membrane bio-systems for sustainable treatment of oil and gas produced water and fracturing flowback water, Sep. Purif. Technol. 171 (2016) 297–311. https://doi.org/10.1016/j.seppur.2016.07.008.

[11] D.J. Miller, X. Huang, H. Li, S. Kasemset, A. Lee, D. Agnihotri, T. Hayes, D.R. Paul, B.D. Freeman, Fouling-resistant membranes for the treatment of flowback water from hydraulic shale fracturing: A pilot study, J. Membr. Sci. 437 (2013) 265–275. https://doi.org/10.1016/j.memsci.2013.03.019.

[12] Md.S. Islam, K. Touati, Md.S. Rahaman, Feasibility of a hybrid membrane-based process (MF-FO-MD) for fracking wastewater treatment, Sep. Purif. Technol. 229 (2019) 115802. https://doi.org/10.1016/j.seppur.2019.115802.

[13] X. Cheng, H. Liang, A. Ding, F. Qu, S. Shao, B. Liu, H. Wang, D. Wu, G. Li, Effects of pre-ozonation on the ultrafiltration of different natural organic matter (NOM) fractions: Membrane fouling mitigation, prediction and mechanism, J. Membr. Sci. 505 (2016) 15–25. https://doi.org/10.1016/j.memsci.2016.01.022.

[14] Y.G. Park, Effect of ozonation for reducing membrane-fouling in the UF membrane,

Desalination 147 (2002) 43–48. https://doi.org/10.1016/S0011-9164(02)00574-X.

[15] S.G. Lehman, L. Liu, Application of ceramic membranes with pre-ozonation for treatment of secondary wastewater effluent, Water Res. 43 (2009) 2020–2028. https://doi.org/10.1016/j.watres.2009.02.003.

[16] S.K. Singh, C.M. Moody, T.G. Townsend, Ozonation pretreatment for stabilized landfill leachate high-pressure membrane treatment, Desalination 344 (2014) 163–170. https://doi.org/10.1016/j.desal.2014.03.011.

[17] D. Wei, Y. Tao, Z. Zhang, X. Zhang, Effect of pre-ozonation on mitigation of ceramic UF membrane fouling caused by algal extracellular organic matters, Chem. Eng. J. 294 (2016) 157–166. https://doi.org/10.1016/j.cej.2016.02.110.

[18] S. Tang, Z. Zhang, X. Zhang, New insight into the effect of mixed liquor properties changed by pre-ozonation on ceramic UF membrane fouling in wastewater treatment, Chem. Eng. J. 314 (2017) 670–680. https://doi.org/10.1016/j.cej.2016.12.032.

[19] H. Wang, M. Park, H. Liang, S. Wu, I.J. Lopez, W. Ji, G. Li, S.A. Snyder, Reducing ultrafiltration membrane fouling during potable water reuse using pre-ozonation, Water Res. 125 (2017) 42–51. https://doi.org/10.1016/j.watres.2017.08.030.

[20] H. Vatankhah, C.C. Murray, J.W. Brannum, J. Vanneste, C. Bellona, Effect of pre-ozonation on nanofiltration membrane fouling during water reuse applications, Sep. Purif. Technol. 205 (2018) 203–211. https://doi.org/10.1016/j.seppur.2018.03.052.

[21] J.L. Bradshaw, N. Ashoori, M. Osorio, R.G. Luthy, Modeling Cost, Energy, and Total Organic Carbon Trade-Offs for Stormwater Spreading Basin Systems Receiving Recycled Water Produced Using Membrane-Based, Ozone-Based, and Hybrid Advanced Treatment Trains, Environ. Sci. Technol. 53 (2019) 3128–3139. https://doi.org/10.1021/acs.est.9b00184.

[22] Y. Lu, Z. He, Mitigation of Salinity Buildup and Recovery of Wasted Salts in a Hybrid Osmotic Membrane Bioreactor–Electrodialysis System, Environ. Sci. Technol. 49 (2015) 10529–10535. https://doi.org/10.1021/acs.est.5b01243.

[23] N.C. Nguyen, H.T. Nguyen, S.-S. Chen, H.H. Ngo, W. Guo, W.H. Chan, S.S. Ray, C.-W. Li, H.-T. Hsu, A novel osmosis membrane bioreactor-membrane distillation hybrid system for wastewater treatment and reuse, Bioresour. Technol. 209 (2016) 8–15. https://doi.org/10.1016/j.biortech.2016.02.102.

[24] W. Luo, F.I. Hai, W.E. Price, W. Guo, H.H. Ngo, K. Yamamoto, L.D. Nghiem, Phosphorus and water recovery by a novel osmotic membrane bioreactor–reverse osmosis system, Bioresour. Technol. 200 (2016) 297–304. https://doi.org/10.1016/j.biortech.2015.10.029.

[25] S. Phuntsho, S. Hong, M. Elimelech, H.K. Shon, Forward osmosis desalination of brackish groundwater: Meeting water quality requirements for fertigation by integrating nanofiltration, J. Membr. Sci. 436 (2013) 1–15. https://doi.org/10.1016/j.memsci.2013.02.022.

[26] S. Phuntsho, H.K. Shon, S. Hong, S. Lee, S. Vigneswaran, A novel low energy fertilizer driven forward osmosis desalination for direct fertigation: Evaluating the performance of fertilizer draw solutions, J. Membr. Sci. 375 (2011) 172–181. https://doi.org/10.1016/j.memsci.2011.03.038.

[27] S. Phuntsho, H.K. Shon, T. Majeed, I. El Saliby, S. Vigneswaran, J. Kandasamy, S. Hong, S. Lee, Blended Fertilizers as Draw Solutions for Fertilizer-Drawn Forward Osmosis Desalination, Environ. Sci. Technol. 46 (2012) 4567–4575. https://doi.org/10.1021/es300002w.

[28] Y. Kim, L. Chekli, W.-G. Shim, S. Phuntsho, S. Li, N. Ghaffour, T. Leiknes, H.K. Shon, Selection of suitable fertilizer draw solute for a novel fertilizer-drawn forward osmosis–anaerobic membrane bioreactor hybrid system, Bioresour. Technol. 210 (2016) 26–34. https://doi.org/10.1016/j.biortech.2016.02.019.

[29] G.S. Arcanjo, F.C.R. Costa, B.C. Ricci, A.H. Mounteer, E.N.M.L. De Melo, B.F. Cavalcante, A.V. Araújo, C.V. Faria, M.C.S. Amaral, Draw solution solute selection for a hybrid forward osmosis-membrane distillation module: Effects on trace organic compound rejection, water flux and polarization, Chem. Eng. J. 400 (2020) 125857. https://doi.org/10.1016/j.cej.2020.125857.

[30] N. Duc Viet, S.-J. Im, A. Jang, Characterization and control of membrane fouling during dewatering of activated sludge using a thin film composite forward osmosis membrane, J. Hazard. Mater. 396 (2020) 122736. https://doi.org/10.1016/j.jhazmat.2020.122736.

[31] J. Yun, C. Cui, S. Zhang, J. Zhu, C. Peng, H. Cai, X. Yang, R. Hou, Use of headspace GC/MS combined with chemometric analysis to identify the geographic origins of black tea, Food Chem. 360 (2021) 130033. https://doi.org/10.1016/j.foodchem.2021.130033.

[32] N.D. Viet, D. Jang, Y. Yoon, A. Jang, Enhancement of membrane system performance using artificial intelligence technologies for sustainable water and wastewater treatment: A critical review, Crit. Rev. Environ. Sci. Technol. 52 (2022) 3689–3719. https://doi.org/10.1080/10643389.2021.1940031.

[33] A. Butkovskyi, A.-H. Faber, Y. Wang, K. Grolle, R. Hofman-Caris, H. Bruning, A.P. Van Wezel, H.H.M. Rijnaarts, Removal of organic compounds from shale gas flowback water, Water Res. 138 (2018) 47–55. https://doi.org/10.1016/j.watres.2018.03.041.

[34] P. Liu, Y. Ren, W. Ma, J. Ma, Y. Du, Degradation of shale gas produced water by

magnetic porous MFe2O4 (M = Cu, Ni, Co and Zn) heterogeneous catalyzed ozone, Chem. Eng. J. 345 (2018) 98–106. https://doi.org/10.1016/j.cej.2018.03.145.

[35] H. Zhang, Z. Xiong, F. Ji, B. Lai, P. Yang, Pretreatment of shale gas drilling flowback fluid (SGDF) by the microscale Fe-0/persulfate/O-3 process (mFe(0)/PS/O-3), Chemosphere 176 (2017) 192–201. https://doi.org/10.1016/j.chemosphere.2017.02.122.

[36] P. Tang, B. Liu, Y. Zhang, H. Chang, P. Zhou, M. Feng, V.K. Sharma, Sustainable reuse of shale gas wastewater by pre-ozonation with ultrafiltration-reverse osmosis, Chem. Eng. J. 392 (2020) 123743. https://doi.org/10.1016/j.cej.2019.123743.

[37] Z. Li, C. Wu, J. Huang, R. Zhou, Y. Jin, Membrane Fouling Behavior of Forward Osmosis for Fruit Juice Concentration, Membranes 11 (2021) 611. https://doi.org/10.3390/membranes11080611.

[38] F. Yang, Z. Huang, J. Huang, C. Wu, R. Zhou, Y. Jin, Tanning Wastewater Treatment by Ultrafiltration: Process Efficiency and Fouling Behavior, Membranes 11 (2021) 461–461. https://doi.org/10.3390/membranes11070461.

[39] M. Xiao, S. Liu, W. Qi, Y. Peng, Q. Yan, H. Mao, Combination tanning mechanism inspired environmentally benign catalyst for efficient degradation of tetracycline, Collagen Leather 5 (2023) 22. https://doi.org/10.1186/s42825-023-00130-w.

[40] S.M.S. Mousavi, R. Dehghanzadeh, S.M. Ebrahimi, Comparative analysis of ozonation (O3) and activated carbon catalyzed ozonation (ACCO) for destroying chlorophyll a and reducing dissolved organic carbon from a eutrophic water reservoir, Chem. Eng. J. 314 (2017) 396–405. https://doi.org/10.1016/j.cej.2016.11.159.

[41] B. Liu, F. Qu, H. Yu, J. Tian, W. Chen, H. Liang, G. Li, B. Van der Bruggen, Membrane Fouling and Rejection of Organics during Algae-Laden Water Treatment Using Ultrafiltration: A Comparison between in Situ Pretreatment with Fe(II)/Persulfate and Ozone, Environ. Sci. Technol. 52 (2018) 765–774. https://doi.org/10.1021/acs.est.7b03819.

[42] A.T. Pikkarainen, S.J. Judd, J. Jokela, L. Gillberg, Pre-coagulation for microfiltration of an upland surface water, Water Res. 38 (2004) 455–465. https://doi.org/10.1016/j.watres.2003.09.030.

[43] P.C. Sangave, P.R. Gogate, A.B. Pandit, Combination of ozonation with conventional aerobic oxidation for distillery wastewater treatment, Chemosphere 68 (2007) 32–41. https://doi.org/10.1016/j.chemosphere.2006.12.053.

[44] S.N. Malik, P.C. Ghosh, A.N. Vaidya, S.N. Mudliar, Catalytic ozone pretreatment of complex textile effluent using Fe2+ and zero valent iron nanoparticles, J. Hazard. Mater.

357 (2018) 363–375. https://doi.org/10.1016/j.jhazmat.2018.05.070.

[45] W. Chen, P. Westerhoff, J.A. Leenheer, K. Booksh, Fluorescence excitation - Emission matrix regional integration to quantify spectra for dissolved organic matter, Environ. Sci. Technol. 37 (2003) 5701–5710. https://doi.org/10.1021/es034354c.